Insulating antiferromagnetism in VTe
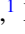
David S. Parker,[1] Li Yin,[1] German D. Samolyuk,[1] Liurukara D. Sanjeewa ●,[1] Xiaoping Wang ●,[2] Valentino R. Cooper ●,[1] Yaohua Liu,[2] Sergey Bud'ko,[3] and Athena S. Sefat ●[1]

[1]*Materials Science and Technology Division, Oak Ridge National Laboratory, 1 Bethel Valley Rd., Oak Ridge, Tennessee 37831, USA*
[2]*Neutron Scattering Division, Oak Ridge National Laboratory, 1 Bethel Valley Rd., Oak Ridge, Tennessee 37831, USA*
[3]*Ames Laboratory and Department of Physics and Astronomy, Iowa State University, Ames, Iowa 20011, USA*

We report a detailed theoretical and experimental study on the vanadium monotelluride VTe, which crystallizes in the NiAs hexagonal structure. First-principles calculations reveal a complex hierarchy of magnetic interactions and energy scales, with the ground state theoretically determined as an $(\frac{1}{2}, 0, \frac{1}{2})$ antiferromagnetic ordering with insulating character and a band gap of 0.5 eV. Experimental synthesis and characterization efforts find a substantially off-stoichiometric orthorhombic structure (a defect NiAs structure) with composition $V_{0.85}Te$, and an apparent Néel point of some 45 K. First-principles calculations find good agreement with the observed Néel point. We also give an extended examination of the effects of off-stoichiometry on the calculated energetics, finding significant volume-related effects. Our first-principles calculations find the stoichiometric phase VTe to have a negative vanadium defect formation energy of over 1 eV, thus explaining the formation of the off-stoichiometric phase. Finally, we provide a structural explanation for the formation of defect structures in this and numerous other NiAs-structure materials.

I. INTRODUCTION

Vanadium—element 23 in the periodic table—is well known to generate many varieties of colorful compounds. This characteristic is closely tied to its multiple oxidation states ($+5$, $+4$, $+3$, and $+2$, exceeding that of any $3d$ element save manganese) which in turn derive from the near degeneracy of its three $3d$ electron states, along with its two $4s$ electrons. Vanadium, however, exhibits magnetism much less frequently than the later $3d$ periodic table elements Cr, Mn, Fe, and Co, despite containing the same number of unpaired $3d$ electrons as hcp cobalt. In a certain sense this is surprising, given that the atomic volume of bcc vanadium is some 25% larger than hcp cobalt and one typically associates larger atomic volumes with narrower bands, and therefore higher Fermi level density-of-states and increased magnetic character. As calculated by Janak some four decades ago [1], however, elemental vanadium has a slightly lower Fermi-level DOS $N(E_F)$ and exchange correlation parameter than hcp Co. V thus avoids a magnetic instability, although the large $N(E_F)$ does lead to a comparatively large superconducting T_c of some 5.13 K [2] due to its strengthening of the electron-phonon interaction.

In this work we will discuss our recent theoretical and experimental work on vanadium monotelluride, VTe, which is relatively little known due to its assumption of the less-common vanadium valence $+2$. Some four decades ago, Prasad [3] found antiferromagnetism in VTe at the relatively high temperature of 420 K, and in addition evidence for insulating character given the observation in that work of an extremely large Seebeck coefficient of some 800 μV/K, which greatly exceeds typical metallic thermopowers of less

than 50 μV/K. Our first-principles calculations confirm the antiferromagnetic ground state and insulating character (the calculated band gap is 0.5 eV), and in addition find the antiferromagnetic ordering wave vector to be $(\frac{1}{2}, 0, \frac{1}{2})$. This ordering wave vector is sixfold degenerate in the magnetic Brillouin zone and is thus suggestive of nematic character, similarly to the parent compounds of the iron-based superconductors.

Although the monotelluride stoichiometry is difficult to attain experimentally, we find that a somewhat off-stoichiometric sample of composition $V_{0.85}Te$ does show indications of magnetic order, although at a much lower temperature, approximately 45 K, than the 420 K posited previously from an anomaly in magnetization data [3]. This suggests that the magnetic order is highly composition dependent, and in addition that suitably off-stoichiometric samples may have magnetic order suppressed to $T = 0$. This would be a "self-doping" unlike that of the iron-based superconductors (FeTe excepted), and it is possible, though clearly unproven, that superconductivity could occur in such samples.

The rest of this paper is organized as follows. In the next three sections we describe the first-principles calculations methods and results on the stoichiometric and defect structures, followed by a detailed description of the experimental results, and a description of the calculated energetics of the defect structures. In the last section we present a conclusion.

II. FIRST-PRINCIPLES CALCULATIONS OF MAGNETISM: METHODS

Our first-principles calculations on stoichiometric VTe are performed using the all-electron, linearized augmented

plane-wave (LAPW) density functional theory code WIEN2K [4], using the generalized gradient approximation (GGA) of Perdew, Burke, and Ernzerhof [5], in the experimental structure of Sondermann [6]. Sphere radii of 2.46 and 2.5 bohrs were used for V and Te, respectively, and an RK_{max} of 9.0 was used, where RK_{max} is the product of the smallest sphere radius and the largest plane-wave expansion wave vector. All calculations used a minimum of 1000 k points in the relevant full Brillouin zone. Spin-orbit coupling was not included, and no internal coordinate relaxation was performed as there are no nonsymmetry dictated coordinates in the NiAs structure.

Since experimentally the samples form in a somewhat vanadium-deficient stoichiometry, we have also conducted substantial numbers of additional calculations. Since vanadium deficiency affects both the unit cell volume and content, we have endeavored to isolate these two effects by performing stoichiometric calculations at the two different volumes reported in the literature [6,7], of 77.21 and 84.26 Å^3 per unit cell. Note that these volumes differ by some 8%. The larger volume hexagonal structure is in fact rather consistent (in terms of effective lattice constants, taking into account the effective symmetry reduction of the defect structure) with our experimental orthorhombic $V_{0.85}$Te. Given this, it is rather likely that the early studies on VTe were studying samples that were also vanadium deficient, but did not have sufficient x-ray diffraction resolution to estimate an effective occupancy or lower-symmetry structure than the stoichiometric NiAs structure. Our calculations of the stoichiometric structure should be considered in this light. We report calculated exchange interactions for both stoichiometric structures from the all-electron calculations and discuss this below.

Given the experimental off-stoichiometry, we have also performed large numbers of all-electron calculations in a V_7Te_8 or $V_{0.875}$Te cell of orthorhombic symmetry, close to the actual $V_{0.85}$Te stoichiometry. Given the seven vanadium atoms in this cell, there is no collinear magnetic state of zero net magnetic moment, so we have considered all possible magnetic states with four vanadium moments in one direction and three in the opposite direction. Due to the myriad of exchange interactions in these calculations, we make no attempt to determine them from these calculations, and leave that task to the static linear-response based [8] calculations described below. In general these all-electron calculations tend to confirm the tendency of the stoichiometric structure to have nearest- and next-nearest-neighbor V-V interactions that are antiferromagnetic.

For a more detailed examination of the exchange interactions, and in particular to calculate the Néel point of the stoichiometric and off-stoichiometric compound, the pair exchange coupling parameters $J_{i,j}$ of the Heisenberg Hamiltonian (1) were obtained using a static linear-response approach [8] implemented within the atomic sphere approximation (ASA) to the Green's function (GF) linear muffin-tin orbital (LMTO) [9] method [10]:

$$H = -\frac{1}{2}\sum_{i,j}{}' J_{i,j}\vec{e}_i\vec{e}_j, \tag{1}$$

where $\vec{e}_i$ is the direction of magnetic moment in lattice site i. Electronic structure has been calculated within density

functional theory approach [11] and local spin density approximation with the von Barth and Hedin [12] parametrization of the electronic exchange-correlation functional. Temperature of magnetic ordering T_c can be estimated within mean field approximation (MFA) using calculated J_{ij} as a maximal solution of following equation:

$$\det\left[\tfrac{1}{3}(J_0)_{nm} - T_c\delta_{n,m}\right] = 0, \tag{2}$$

where $(J_0)_{nm}$ is the effective exchange coupling magnetic moment of V basis atom n with all V basis atoms m. Note that in frustrated systems, such as this one, this mean field approach provides only a rough estimate of the magnetic ordering temperature, a point we will return to in the next section.

III. FIRST-PRINCIPLES CALCULATIONS OF MAGNETISM: RESULTS OF STOICHIOMETRIC STRUCTURE

We begin with the nonmagnetic electronic structure, calculated in the all-electron calculations. Depicted in Fig. 1 (top panel) is the calculated density-of-states (DOS) for this case. Three facts are immediately apparent from this plot: first, nonmagnetic VTe is metallic, given the substantial Fermi level (E_F) density-of-states $N(E_F)$. Second, there is a substantial DOS peak at or near E_F, indicating a propensity for magnetic ordering; and third, nearly all of the spectral weight near E_F is of vanadium character, again suggestive of magnetic order. In fact on a per V basis, $N(E_F)$ is some 6.3/eV, which causes the Stoner product $I·N(E_F)$ to take the value 2.5, far exceeding the unity value at which a magnetic instability occurs in Stoner theory (here we take the exchange correlation parameter for V as 0.4 eV, following Janak [1]). This fact is suggestive, though not conclusive, of strong magnetic order in VTe.

In Fig. 1 (bottom) we show the calculated density-of-states (DOS) in the theoretically determined antiferromagnetic ground state "AF2" (see Fig. 3 for more details on this state) at the smaller volume of 77.21 Å^3. For this calculation only we have used a variant of the GGA known as the "modified Becke-Johnson" potential [13], which was constructed to produce more accurate band gaps than the straight GGA, which generally understates these gaps. Consistent with Prasad's results, we find insulating character with a significant band gap of some 0.5 eV. Both valence and conduction bands are primarily of V character, with the valence band exhibiting the usual spin-up site (V1) and spin-down site (V2) separation into the spin-up and spin-down DOS. While there is some Te weight near the band edges, it is primarily located between 2 and 5 eV below the valence band maximum. The d-orbital resolved DOS (Fig. 1 bottom panel) shows that all 5 V d orbitals contribute significantly to the DOS, suggesting a complexity of electronic states and interactions.

The calculated band structure within the AF2 ground state is shown in Fig. 2. As in the bottom DOS plot, unlike canonical pictures of delineation of d orbitals in terms of e_g and t_{2g} manifolds, directly applicable to compounds such as rocksalt oxides, here we see a notable overlap of all the vanadium d orbitals within both the valence and conduction bands, which is believed to be related to the NiAs hexagonal structure.
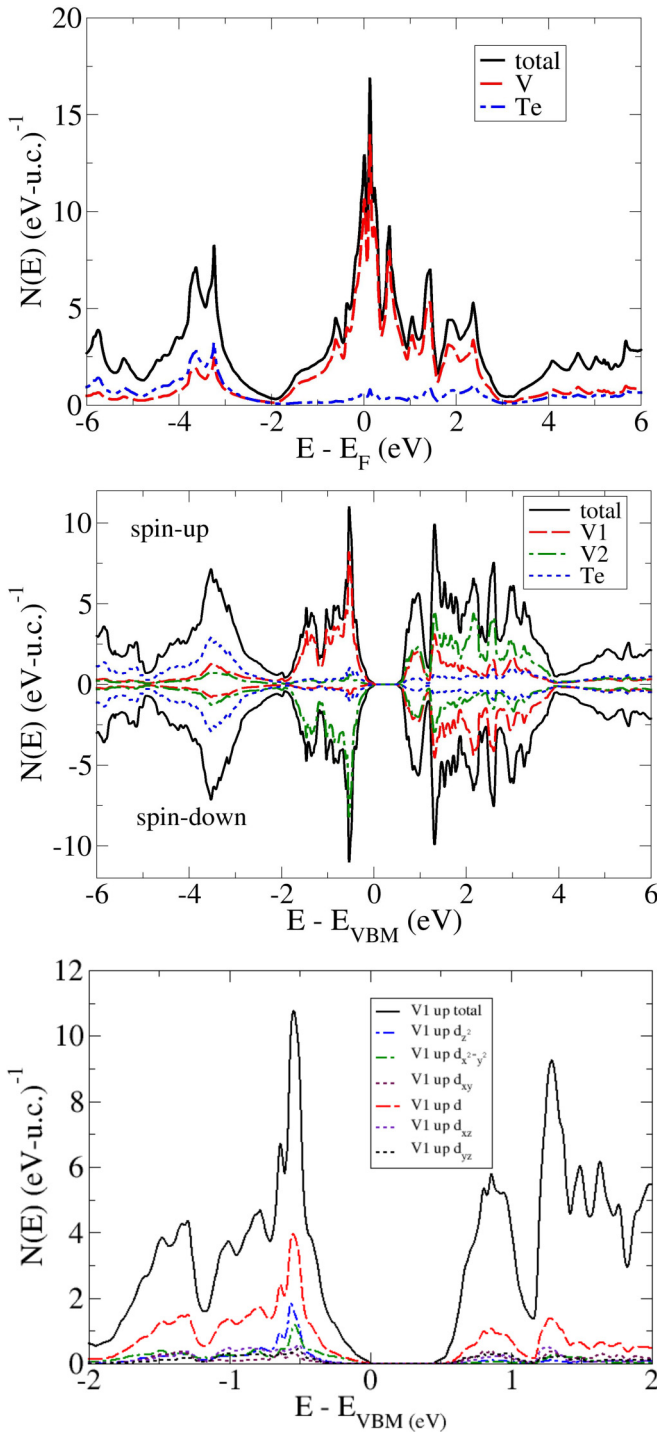
FIG. 1. The calculated nonmagnetic (top) and antiferromagnetic density-of-states (middle) of stoichiometric VTe. Bottom: The near-gap vanadium d-orbital resolved densities-of-states, majority spin V atom.

To gain a better understanding of the magnetic character here we have performed additional spin-polarized calculations on VTe, including a ferromagnetic state, four antiferromagnetic states, and a *ferrimagnetic* state. All these states lie more than 200 meV per vanadium below the nonmagnetic configuration, suggestive of local-moment antiferromagnetism, where it is the energetics of competing magnetic states that

determines the ordering point. In the NiAs structure type the two most important V-V exchange interactions are typically the nearest-neighbor c-axis coupling, with two multiplicity and here a distance of 3.066 Å, and the sixfold next-nearest-neighbor planar V-V interaction, in the smaller cell at a distance of 3.813 Å and at 3.98 Å in the larger. We will see that it is this latter next-nearest-neighbor interaction that is pivotal in determining the magnetic ground state. As indicated in Table I, the simple c-axis antiferromagnetic state (AF1), as observed in numerous materials such as MnTe and MnBi$_2$Te$_4$, falls some 105 meV per vanadium above the ground state AF2 in the smaller cell and 58.2 meV in the larger. In this AF2 ground state, as depicted in Fig. 3, the c-axis nearest neighbors are antialigned, as are four of the planar nearest neighbors, which is the maximum possible "antiferromagnetic" arrangement in this hexagonally frustrated system.

As Table I suggests, AF3 and AF4 are additional antiferromagnetic states: in AF3 the nearest-neighbor c-axis coupling is ferromagnetic and four of the next-nearest-neighbor planar atoms are antiferromagnetically coupled, while in AF4 the c-axis coupling is antiferromagnetic and two of the planar next-nearest neighbors are antiferromagnetically coupled. In the ferrimagnetic FI1 state, six of the eight vanadium atoms in the $2 \times 2 \times 1$ unit cell are aligned and two antialigned.

Already from Table I one sees a substantial volume dependence of the energetics, with all energy values relative to the ground state changing substantially from the 8% larger volume, We see that the energy of the nonmagnetic state nearly doubles from 308 to nearly 550 meV/V, while the relative position of the FM and AF1 states changes. Most strikingly we find that the AF4 state energy reduces to just 18.4 meV/V from 31.0 meV. It is well known that, energetically speaking, closely competing states tend to drive ordering points towards $T = 0$. In particular, the mean field approximation of T_c as a third of this energy difference [14–16] would yield an ordering point of approximately 70 K. Taking into account the fact that MFA usually overestimates transition temperature by ∼30%, the resulting value, 49 K, is very close to the observed 45 K value. We also include for reference calculations, at the larger volume, within a GGA $+ U$ approach with a U value of 2 eV assumed for the V orbitals, which changes the relative order of some of the excited states but leaves the ground state AF2 unchanged.

There are other inferences one may make from the exchange constants presented in Table II. At the larger volume one notes the relative predominance of the nearest-neighbor exchange J_1 at 26.91 meV, with all other exchange constants nearly an order of magnitude smaller. Yet at the smaller volume, the values and distance dependence are rather different—the nearest-neighbor J_1 is less than half as large, while J_2 more than doubles. Note also the effective c-axis frustration from J_1 and J_4 having the same sign. J_4, from Fig. 2, is the interaction connecting two V a full c-axis lattice spacing apart, while J_1 connects V neighbors half as far apart. Since both are strongly antiferromagnetic here, it is not possible to satisfy the system's desire for both pairs of vanadium to be antiferromagnetically aligned. While geometric frustration is of course well known in hexagonal systems, it usually arises from the hexagonal planar arrangement. Here there is an additional c-axis frustration.
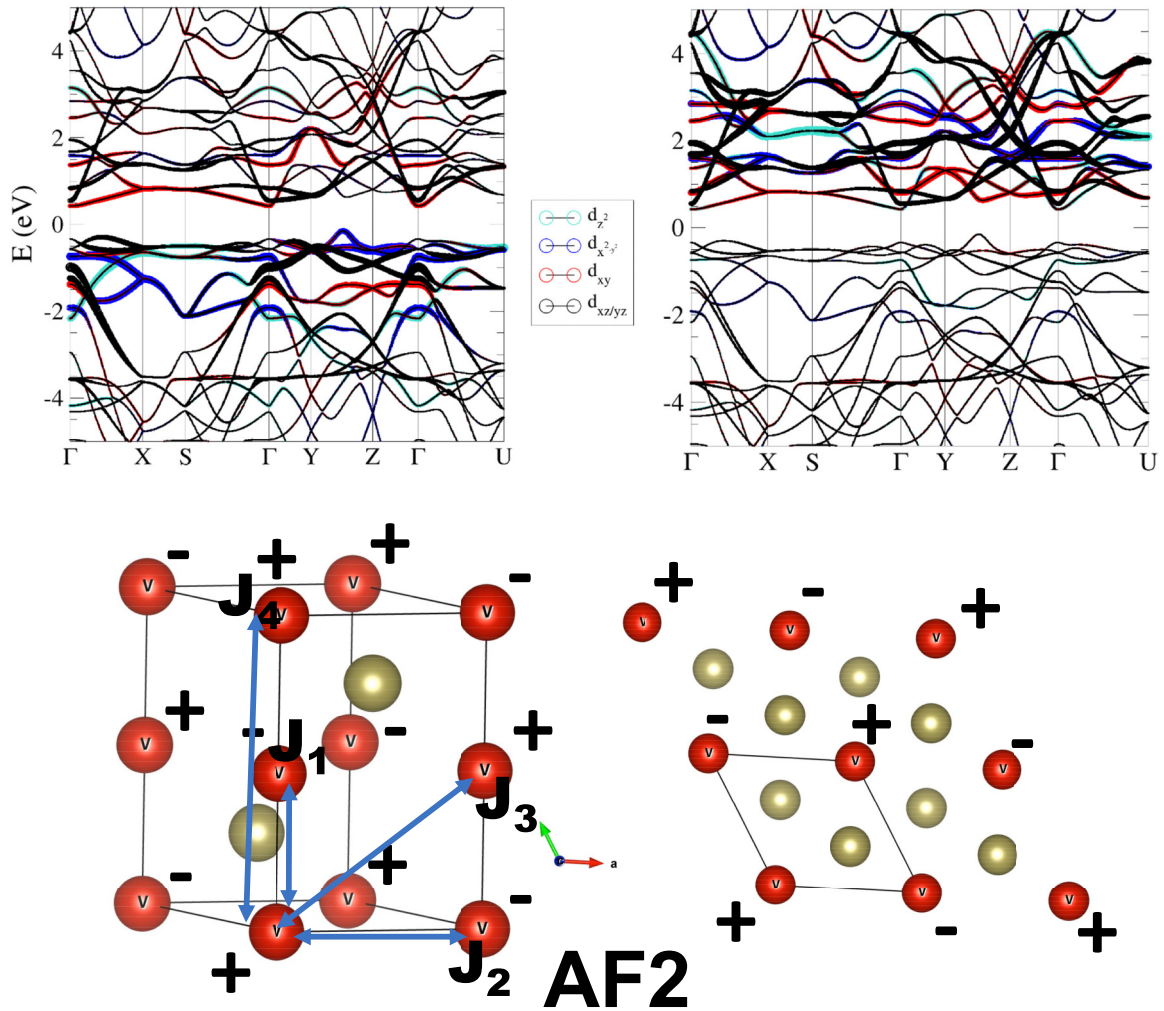
FIG. 2. Top: The band structure within the antiferromagnetic state, with vanadium 3*d* band character indicated. Majority spin is in the left-hand panel and minority on the right. Bottom: the AF2 magnetic structure, with exchange interactions indicated.

Strictly speaking, a large exchange interaction at large distance found from a mapping to a finite-distance Heisenberg model is often an artifact of substantial exchange interactions at still larger distances, neglected in these all-electron calculations. To assess this we turn to the LMTO calculations (performed at the larger volume of 84.26 A^3).

The LMTO calculations for stoichiometric VTe find the same $(\frac{1}{2}, 0, \frac{1}{2})$ ground state as in the all-electron calculations, and in addition permit a more detailed examination of the exchange interactions. For these calculations a 16-atom unit cell, or a $2 \times 2 \times 1$ supercell of the basic two formula unit cell was constructed, and the exchange interactions analyzed as described above. Note that in the Heisenberg mapping employed [Eq. (1)] the absolute value of spin magnetic moment is absorbed into the definition of the J_{ij} so that, as in the all-electron exchange interactions, these are effectively energy differences caused by small deviation of magnetic moments directions on atoms i and j rather than literal exchange interactions. We present results for the former interactions here in Table III.

Table III shows the first three exchange interactions in the LMTO method to be antiferromagnetic, as in Table II, while in contrast the last three are ferromagnetic. Note that

in these calculations we further distinguish two symmetry-separated components of the J_3 described above. We note two salient characteristics of Table III—as previously, there is *c*-axis frustration, but in this case involving the $3/2c$ lattice spacing J_5, whose ferromagnetic nature competes with the antiferromagnetic $1/2c$ spacing J_1. Second, and perhaps most crucially, the exchange interactions show no strong drop off with distance, with the 9.2 Å J_5 essentially as large in magnitude as any other. Such rather unusual behavior has been observed previously in the potential permanent magnet MnBi, where a fifth nearest-neighbor interaction was found of particular importance. The effective exchange coupling J_0, defined as a sum of one specific atom interactions with the rest of magnetic system, is 18.6 meV. J_0 value equals to second derivative in total energy with respect to spin rotation and its positive value guarantees the stability of AF2 ordering. It is worth mentioning that the summation over exchange coupling presented in Table III gives $\sim70\%$ of total J_0, 26 meV. The last value could be calculated by utilizing the "sums rule" [8]. Utilizing expression (2) for magnetic transition temperature we obtain $T_N = 72$ K.

This MFA calculated T_N is very close to value extracted from all-electron calculation, 70 K, and, again, taking into
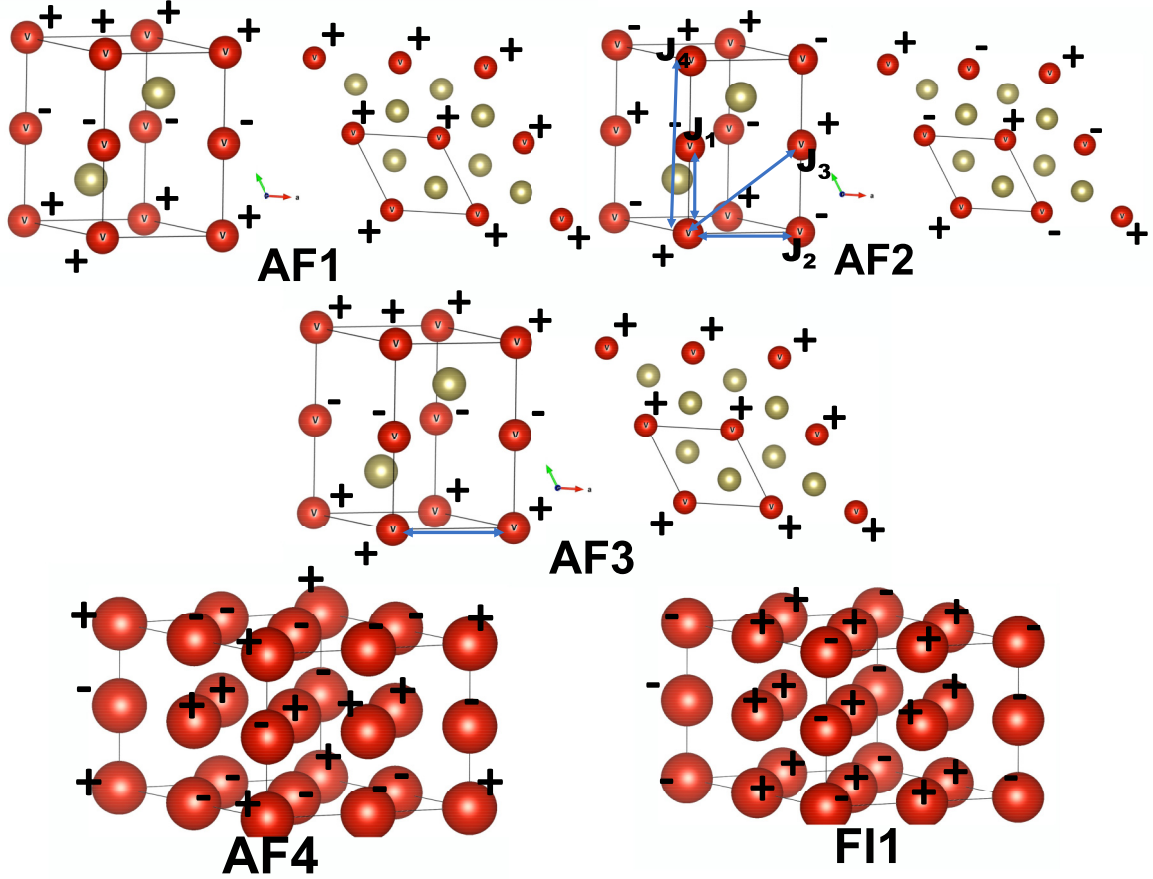
FIG. 3. The first-principles calculated magnetic structures of stoichiometric VTe, with the nearest-neighbor exchange interaction J_1 and next-nearest-neighbor interactions J_2-J_4 indicated in the AF2 plot. Vanadium atoms are in red and tellurium in gray. For simplicity, the Te atoms are not shown for the AF4 and FI1 states.

account that MFA usually overestimates transition temperature by $\approx 30\%$ is rather close to the experimental value 45 K.

IV. FIRST-PRINCIPLES CALCULATIONS OF MAGNETISM: RESULTS OF DEFECT STRUCTURE

As mentioned previously, we have conducted a substantial additional study of the actual off-stoichiometric $V_{0.85}$Te structure, which we model via a 15-atom V_7Te_8 structure of stoichiometry $V_{0.875}$Te. We begin with the all-electron calculations. Depicted in Fig. 4 is the modeled structure, which contains a single vanadium vacancy at the center. Neglecting minor differences in the V-V interatomic distances for the other atoms, we have studied all collinear magnetic structures with four of the seven vanadium of one orientation and the other three of the opposite orientation, the closest magnetic

TABLE I. First-principles, all-electron-calculated properties of magnetic states at 77.26 and 84.26 Å^3 cell unit volume, within the straight GGA, and with a U value of 2 eV applied to the vanadium d orbitals, as indicated. Here NM refers to the nonmagnetic state, FM to the ferromagnetic state, and AF1–AF4 are antiferromagnetic states, while FI1 is a ferrimagnetic state. ΔE refers to the calculated energy relative to the ground state AF2, and m to the magnetic moment within the V LAPW sphere. For the states AF1–AF4, m is a staggered moment, while the nn and nnn coefficients refer to the mapping of the magnetic state energetics to a Heisenberg magnetic model, see the text. The energy values in parentheses refer to values calculated with the somewhat larger cell (volume 84.26 A^3 whose lattice parameters are close to that of the experimental off-stoichiometric compound).

Magnetic state	ΔE_{GGA} (meV/V)	$\Delta E_{\mathrm{GGA}+U_{\mathrm{V}(2\ \mathrm{eV})}}$	$m\ (\mu_B/\mathrm{V})$	nn	nn2	nn3	nn4
NM	308.3 (549.9)	–	–	–	–	–	–
FM	96.1 (118.9)	(184.2)	1.99	2	6	12	2
AF1	104.9 (58.2)	(20.3)	±2.04	−2	6	−12	2
AF2	0 (0)	(0)	±2.10	−2	−2	4	2
AF3	63.3 (121.4)	(165.8)	±1.99	2	−2	−4	2
AF4	31.1 (18.4)	(6.4)	±2.1/2.05	−2	0	0	2
FI1	76.9 (128.3)	(173.2)	+2.00/−1.91	2	0	0	2

TABLE II. Exchange constants (meV) extracted from the all-electron calculations. See Fig. 3 for definitions of these exchange interactions. Positive values denote antiferromagnetic interactions.

Exchange interaction	84.26 Å^3 vol.	77.21 Å^3 vol.
J_1	26.91	11.36
J_2	3.26	8.41
J_3	−1.93	−2.25
J_4	3.87	1.70

states to a truly antiferromagnetic, or zero-moment order. Note that there are $(6 \times 5 \times 4)/3!$, or 20 such structures. The coordinate positions in these structures are identical and were previously optimized within a single, generally antiferromagnetic, structure.

In general, within this manifold of structures, there are energy differences somewhat smaller than in the stoichiometric structures presented previously. The maximum energy difference from the ground state is only 60 meV per vanadium. The magnetic ground state (a state generally equivalent to the AF2 state of the stoichiometric calculations) falls some 20 meV per vanadium beneath a manifold of three nearly degenerate excited states. This is generally consistent with the 18 to 30 meV energetic difference, in the stoichiometric calculations, of the AF4 state relative to the ground state AF2, and so it appears that the evident disorder does not significantly affect the Néel point, other than the related volume effects.

Corroborating this are our LMTO calculations of the ordering point, similar to VTe case we calculated exchange couplings J_{ij} using a linear response approach. It was already mentioned that introduction of V vacancy significantly reduces symmetry of the system. As a result, one class of V magnetic atoms (for the formulation of the Heisenberg Hamiltonian in an AFM system two atoms with opposite magnetic moments have the same set of exchange couplings and could be considered as equivalent) is split into five groups of nonequivalent atoms. This makes analysis of magnetic interactions in this system quite complicated. However, a lot of information about it could be extracted from values of

TABLE III. The largest LMTO-calculated exchange couplings in VTe in meV, as a function of vector $\vec{R}_i - \vec{R}_j$ in units of the $a \times a \times c$ unit cell, corresponding degeneracy g. The convention of the labeling of the exchange interactions J follows those indicated in Fig. 2, rather than those given in Eq. (1). J_{3a} and J_{3b} are symmetry-distinguished components of J_3 in Table II. Positive values indicate antiferromagnetic coupling. Note that the exchange constant magnitudes do not decrease substantially with distance.

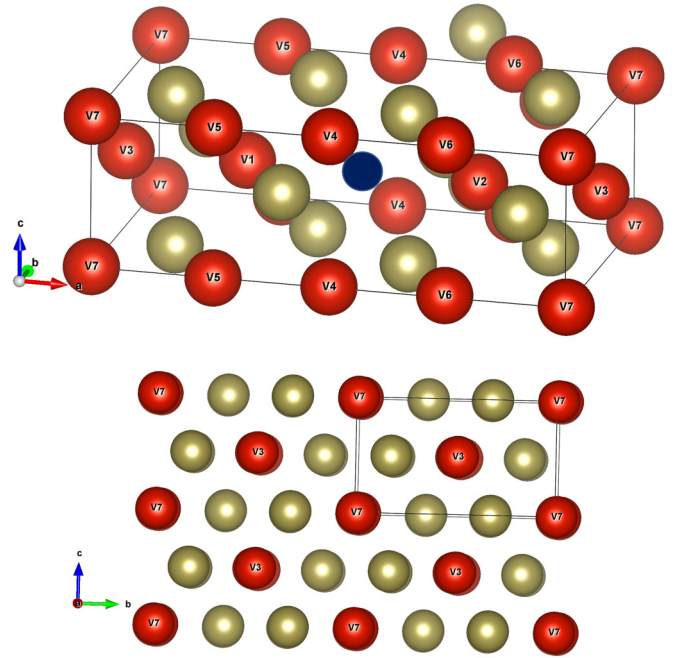| J	g	$|\vec{R}_i - \vec{R}_j|$ (A)	$\vec{R}_i - \vec{R}_j$	$J_{i,j}$
J_1	2	3.064	(0, 0, 1/2)	1.29
J_2	6	3.98	(0, 1, 0)	1.49
J_{3a}	8	5.023	(0,1, 1/2)	3.91
J_{3b}	4	5.023	(1, 1, 1/2)	−3.48
J_4	2	6.128	(0, 0, 1)	−1.44
J_5	2	9.193	(0, 0, 3/2)	−3.69

FIG. 4. A depiction of the V_7Te_8 unit cell used for the defect structure calculations, with axes indicated (note that that the x axis here corresponds to the c axis in the stoichiometric cell). Top: A perspective view showing the entire cell. The blue sphere at the center of the cell indicates the vanadium vacancy. Bottom: A view looking down the x axis, showing in the upper right the orthorhombic axes. The bc orthorhombic plane corresponds to the ab hexagonal plane in the stoichiometric structure.

effective exchange couplings $(J_0)_n$, where n is the indexing type of the V atom, presented in Table IV.

The presence of negative $(J_0)_0$ points out the instability of the current orientation of V_0 magnetic moment and possible existence of lower energy magnetic ordering. A possible approach to finding magnetic ordering minimizing zero temperature energy of the Heisenberg Hamiltonian is to apply Fourier analyses of exchange couplings (for example, see discussion in Ref. [17]). This transformation could be applied to all moments of the system. It corresponds to the modulation of magnetic moment of whole magnetic unit cell by plane wave with propagation vector $\vec{Q}$ from the irreducible part of the Brillouin zone. Or just one type of magnetic moments. Later results in modulation of one type of the atoms magnetic moments only preserving orientation of the rest of the system. The results of these two operations is presented in Fig. 5.

In Fig. 5(a) energy minima corresponds to Γ point, thus, there is no possible modulation of current magnetic cell reducing total energy described by the Hamiltonian (1). However,

TABLE IV. The LMTO-calculated effective exchange couplings $(J_0)_n$ in $V_{0.875}Te$ in meV for five nonequivalent V atoms, $n = 0$–4.

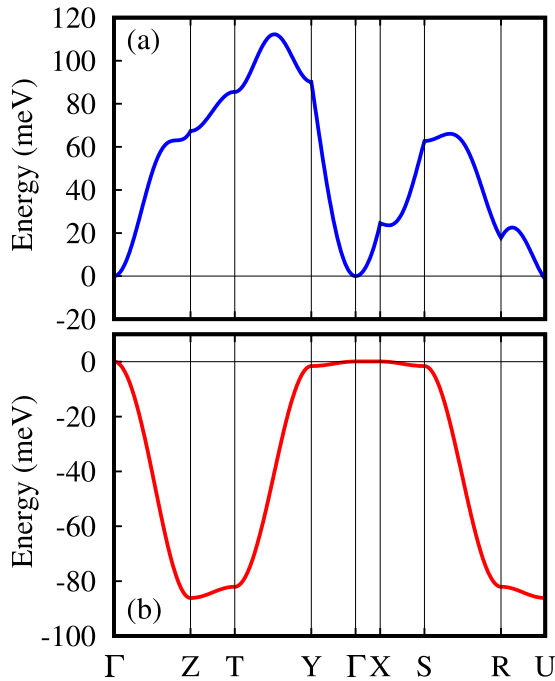| $(J_0)_0$	$(J_0)_1$	$(J_0)_2$	$(J_0)_3$	$(J_0)_4$
-4.49	22.58	38.62	30.33	24.48

FIG. 5. Zero temperature energy of the Heisenberg Hamiltonian with calculated J_{ij} as a function of plane wave magnetic moment modulation with propagation vector $\vec{Q}$ applied to whole moments (a), and moments of V_0 atoms only (b). The $\vec{Q}$ dependence is shown along high symmetry direction in the irreducible part of the Brillouin zone.

FIG. 6. (a) Projected view of $V_{0.85}$Te structure showing the stacking of V-Te-V along the a axis together with $V_{0.85}$Te grown single crystals. (b) Stacking of 2D vanadium layers alternating along the a axis. Each layer has two crystallographically different V sites.

the modulation with any $\vec{Q}$ along Γ-Z, Z-T, T-Y, S-R, and R-U direction applied to magnetic moment of V_0 atom reduces the energy, Fig. 5(b). This is an expected result, since, corresponding $(J_0)_0$ is negative, i.e., divination from the original direction should reduce system energy. To verify this prediction we executed LMTO calculation of the system with doubled along the z-direction cell and changing orientation of V_0 atom moments layer by layer along z. The magnetic moment orientation of the rest of the V atoms is preserved. These magnetic configuration correspond to modulation presented in Fig. 5(b) in Z point. It was obtained that the total energy of the modulated structure is slightly higher, by ~18 meV per V_0 atoms. A possible reason for this discrepancy is that exchange coupling J_{ij} is calculated for a small deviation from a particular magnetic ordering and does not reflect energetics of the system with a completely flipped half of V_0 magnetic moment. Thus, according to the obtained result, the corresponding magnetic moments even at zero temperature deviates from the original collinear orientation, but do not necessarily "flip."

V. EXPERIMENTAL SYNTHESIS AND CHARACTERIZATION MEASUREMENTS

As already mentioned, we have conducted experimental synthesis and characterization work in an attempt to observe and describe the robust magnetism predicted theoretically. Our samples form somewhat off-stoichiometry (a fact explained in the following section), and we have studied in
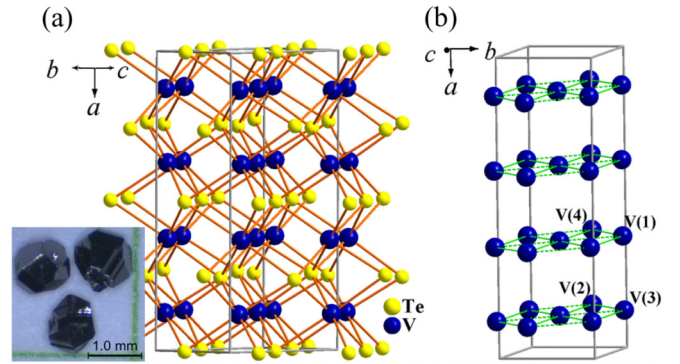
detail a sample whose composition we find from EDX and site-occupancy refinement in diffraction to be $V_{0.85}$Te. In Fig. 6 we show the physical structure of this sample, which forms in an orthorhombic structure (the usual lower-symmetry structure to a hexagonal structure [18]) that is essentially a defect NiAs structure, with several partially occupied sites.

As Fig. 6 indicates, this is a rather three-dimensional structure, just as in the stoichiometric NiAs structure and as in the hexagonal iron chalcogenides [19], which also form in the NiAs structure. This structural similarity makes it plausible that despite the significant off-stoichiometry, this sample should show some vestiges of the magnetism that appears so prominently in the theoretical calculations.

To test this, we have conducted measurements of the magnetic susceptibility $\chi(T)$, both in field-cooled and zero-field-cooled configurations, under an applied field of 1 T. We show the results of these measurements in Fig. 7(a). There we observe a susceptibility which increases slowly as the temperature is reduced from 700 to 100 K. Beginning at 100 K, $\chi(T)$ begins to increase more rapidly, and exhibits a fairly well-defined maximum at 45 K, before decreasing thereafter. Such a maximum indicates an antiferromagnetic ordering, although without detailed information on this ordering.

Adding support to this observation is the measured specific heat, presented in Fig. 7(b). There one sees a feature at 45 K (the feature is more clearly visible in the inset, where we plot the temperature derivative of the specific heat). That this feature appears at essentially the same temperature as the $\chi(T)$ feature is in our view strong evidence for long-range magnetic order, which our theoretical work argues as deriving from an antiferromagnetic ordering.

In Fig. 8 we also present the pressure dependence of the Néel point, which is substantial, dropping significantly for small pressures of just 14 kbar, or 1.4 GPA. This is consistent with the previous theoretical results showing a substantial volume dependence of the exchange interactions, which would correspondingly affect the Néel point.

We have attempted, without success, to observe (via the Spallation Neutron Source—see the Appendix) the actual magnetic structure in this sample, by searching at a comparatively wide range of wave vectors, including that found
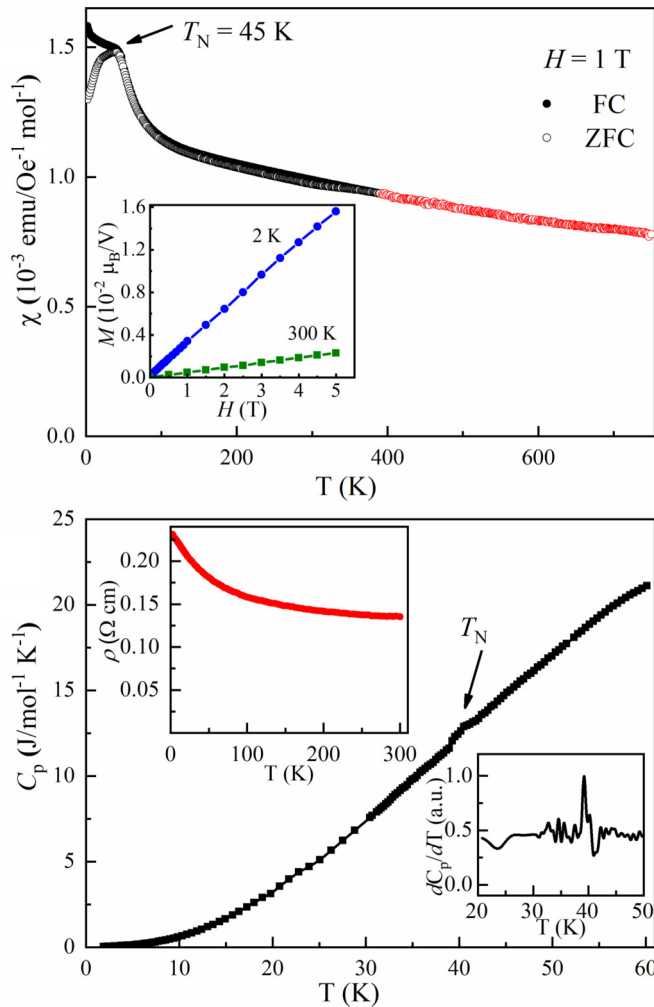
FIG. 7. (a) Temperature dependence of magnetic susceptibility $\chi(T)$ for $V_{0.85}Te$; the inset depicts a linear field dependence of magnetization, $M(H)$, at 2 and 300 K. (b) Heat capacity for $V_{0.85}Te$; the upper inset shows the temperature dependence of the electrical resistivity $\rho(T)$ and the lower inset the temperature derivative of the heat capacity.

FIG. 8. Pressure dependence of the Néel point of $V_{0.85}Te$. The dotted line through the data is a guide to the eye.

VI. DEFECT ENERGY CALCULATIONS

Since the robust magnetic order observed in our all-electron first-principles calculations is substantially reduced by the vanadium off-stoichiometry, it is of interest to consider the origin of this off-stoichiometry. To do this we have studied the neutral vacancy formation energy for both V and Te, using 16-atom unit cells. All calculations were performed with the Vienna *ab initio* simulation package (VASP) [20–23] employing projector augmented wave (PAW) potentials with a plane-wave cutoff of 500 eV and valence electronic configurations of V: $3s2\ 3p6\ 3d3\ 4s2$ and Te: $5s2\ 5p4$. To account for exchange and correlation effects the Perdew-Burke-Erzenhof functional modified for solids (PBEsol) [24] was used. To account for strong correlations we employed a simplified rotationally invariant Hubbard U parameter of 2 eV. Where possible, we investigated up to four different AFM orderings and report the defect formation energies only of the lowest energy configuration. We computed the neutral defect formation energies ($\Delta E_{\text{vacancy}}$) as follows:

$$\Delta E_{\text{vacancy}} = E_{V_{8-n}Te_{8-m}} + nE_V + mE_{Te} - 8E_{VTe}, \qquad (3)$$

where $E_{V_{8-n}Te_{8-m}}$ is the total energy of the defect unit cell with n V atoms and m Te vacancies (where n, m ranges from 0 to 2). E_V and E_{Te} are the total energies per atom of bulk V and Te in their ground states, while E_{VTe} is the total energy of bulk, defect-free VTe per formula unit. In all cases we relaxed the internal atomic coordinates and lattice constants with a force convergence criteria of 0.01 eV/Å. For the bulk VTe we find a ground state configuration of AFM *A* type, which differs from the magnetic ground-state AF2 found in the all-electron calculations. This may be related to the relaxation of the internal atomic coordinates and the lattice constants.

In any case, as indicated in Fig. 9, while Te vacancies have almost universally a large positive formation energy, for the cells with 1 and even 2 V vacancies (and no Te vacancies)

from theory in the stoichiometric structure (translated to orthorhombic coordinates). As the preceding paragraph suggests, this lack of success is likely due to the complexity of the exchange interactions in the defect structure, and thereby the great difficulty in theoretically predicting the magnetic order in this sample.

We have also measured the resistivity $\rho(T)$ of this sample, which we present in the inset of Fig. 7(b). It is largely T independent, rising slowly from a value of 0.15 mΩ cm at 750 K to approximately 0.23 mΩ cm as T approaches zero. This T independence of $\rho(T)$ is consistent with the large numbers of partially occupied sites in the defect structure, which yield a largely T-independent electronic scattering time τ. That $\rho(T)$ decreases slightly with increasing temperature (or "semiconducting" behavior) may be evidence of the likely semiconductivity of the stoichiometric phase, although with such large numbers of vanadium vacancies it is difficult to make this argument rigorous.
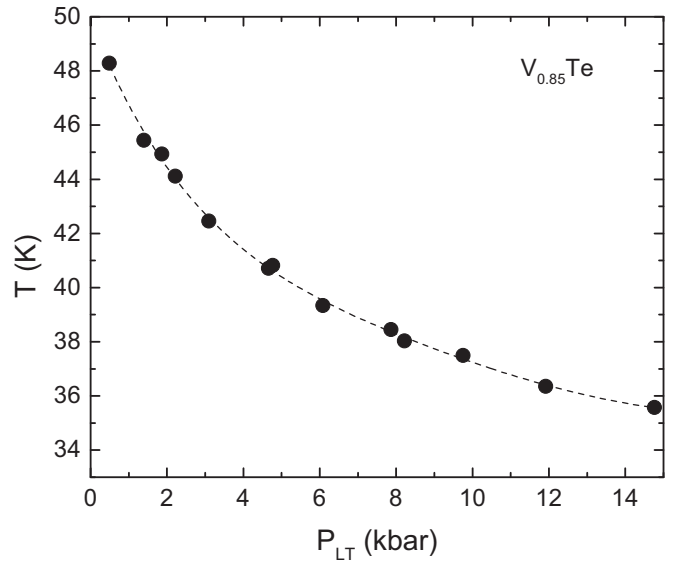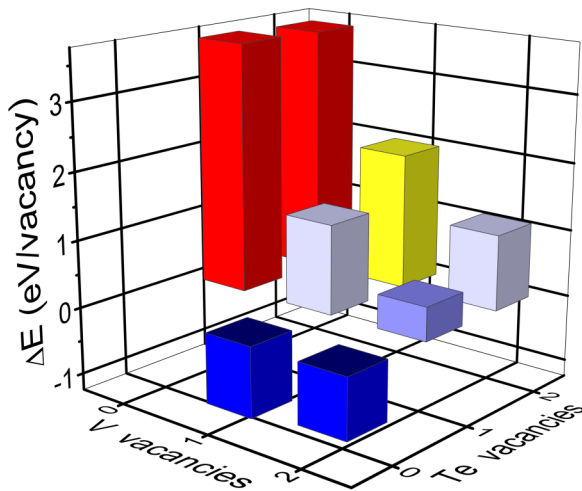
FIG. 9. The first-principles-calculated neutral defect formation energy, for the number of V and/or Te defects indicated on the axes (in a 16-atom unit cell). Note the generally large positive energies associated with tellurium vacancies, indicating the likely stoichiometry of this sublattice, and the large negative energies—more than 1 eV—associated with both 1 and 2 vanadium vacancies per cell. These substantial negative energies suggest a strong propensity for vanadium vacancies to form, consistent with the vanadium deficiencies observed in our $V_{0.85}Te$ sample.

substantial negative energies exceeding 1 eV in magnitude are found, indicating the energetic favorability of V vacancies. This is completely consistent with the observed 15% vanadium deficiency in our $V_{0.85}Te$ sample.

It is of interest to consider the atomic origin of this behavior. Vanadium and tellurium have substantially different electronegativity, with the electronegativity of V estimated [25] as relatively low at 1.63, while that of Te is considered elsewhere to be much larger at 2.2. This clearly contributes significantly to the insulating character depicted in Fig. 1 as found in Prasad's experiment, even well above the presumed 420 K ordering point. Thus Te is considered an electron acceptor and V an electron donor.

One may also consider that in an insulating configuration, higher valence states are more common and more energetically favorable. Indeed, in the V-Te phase diagram there are at least two compounds with smaller V proportion than VTe— V_3Te_4 [26] and VTe_2. The latter compound can reasonably be presumed to have a +4 valence for V. V vacancies, as we find experimentally and theoretically here, will tend to increase the effective charge state here. Finally, there is likely a *structural* reason for the ready formation of V vacancies here. In the NiAs structure (depicted in Fig. 2) the 3d element (in this case V) has a rather close V neighbor along the c axis at 3.066 Å. It is not hard to imagine that this is energetically unfavorable, given an equivalent charge state of these two atoms, which would thus tend to repel one another. A substantial number of V vacancies reduce this energy cost. Note that there are numerous other NiAs structure transition metal chalcogenides, such as CrS [27], CrTe [28], FeS, FeSe [29], and FeTe [30], which also exhibit 3d atom vacancy structures. In keeping with this line of reasoning, one can see that one would not expect Te vacancies in this structure, since the Te atom has six V nearest neighbors (of opposite valence) in a symmetric octahedral configuration, which thus stabilize its stoichiometric state.

VII. CONCLUSION

To summarize, we have conducted a comprehensive theoretical and experimental study of NiAs structure VTe, for which antiferromagnetism was found several decades ago. We confirm, from both theory and experiment, the antiferromagnetism, though at a much lower temperature than found previously. In addition we find that, as with numerous NiAs structure chalcogenides, the material forms substantially off-stoichiometry, a fact which we explain as arising from the combination of an unfavorable V valence of +2, a substantial electronegativity difference between V and Te, and the NiAs structure itself.

APPENDIX: SINGLE CRYSTAL NEUTRON DIFFRACTION WORK

Single-crystal neutron diffraction experiments at temperatures between 6 and 600 K were carried out at the CORELLI spectrometer [32] at the Spallation Neutron Source (SNS). CORELLI is a quasi-Laue time-of-flight instrument and the incident neutron energy band between 10 and 200 meV was used during the experiment. CORELLI is equipped with a large 2D detector, with a $-20°$ to $+150°$ in-plane coverage and $\pm 28°$ out-of-plane coverage, making it very efficient to

search for features over a large reciprocal space. The size of the crystal used in the experiments is about $1 \times 1 \times 1$ mm^3. The data were collected during two separated runs below and above 300 K, respectively, using different setups. The data were collected at 6 and 60 K for the first run, and were collected at 300, 500, and 600 K during the second run. The temperatures were selected to be below and above the two potential magnetic transition temperatures. The first one is 45 K as found in the magnetic susceptibility data, and the second one is 420 K as previously reported [3]. Experiments were conducted by rotating the sample through a 180° range with a 2° step at each temperature. The Mantid package was used for data reduction including Lorentz and spectrum corrections [33]. The integrated Bragg intensities were obtained from integration in the 3D reciprocal space and were corrected for background.

By comparing the data collected at 6 and 60 K, as well as the data collected at 300, 500, and 600 K, no new Bragg-peaklike features have been found. We have also compared the Bragg peak intensity and have not found any significant enhancement in peak intensities when the sample temperature decreased from 60 to 6 K, and from 600 to 300 K. To directly compare the peak intensity below and above 300 K turns out to be less reliable because different sample mounts and sample environment settings were employed. Since there is a clear anomaly in the magnetic susceptibility data, such a null result may suggest that the ordered magnetic moment is much less than the predicted value.

---

[1] J. F. Janak, Uniform susceptibilities of metallic elements, Phys. Rev. B **16**, 255 (1977).

[2] A. Wexler and W. S. Corak, Superconductivity of vanadium, Phys. Rev. **85**, 85 (1952).

[3] C. Prasad and R. A. Singh, Magnetic and electrical transport properties of vanadium telluride, Z. Naturforschung A **35**, 701 (1980).

[4] P. Blaha, K, Schwarz, G. Madsen, D, Kvasnicka and J. Luitz, *WIEN2k, An Augmented Plane Wave + Local Orbitals Program for Calculating Crystal Properties* (K. Schwarz, Tech. Univ. Wien, Austria, 2001).

[5] J. P. Perdew, K. Burke, and M. Ernzerhof, Generalized Gradient Approximation Made Simple, Phys. Rev. Lett. **77**, 3865 (1996).

[6] U. Sondermann. Z. Angew. Phys. **30**, 41 (1970).

[7] P. Ehrlich, Ueber Titanselenide und telluride, Z. Anorg. Allgem, Chem. **260**, 1 (1949).

[8] A. Liechtenstein, M. I. Katsnelson, V. P. Antropov, and V. A. Gubanov, Local spin density functional approach to the theory of exchange interactions in ferromagnetic metals and alloys, J. Magn. Magn. Mater. **67**, 65 (1987).

[9] O. K. Andersen, Z. Pawlowska, and O. Jepsen, Illustration of the linear-muffin-tin-orbital tight-binding representation: Compact orbitals and charge density in Si, Phys. Rev. B **34**, 5253 (1986).

[10] M. van Schilfgaarde and V. P. Antropov, First-principles exchange interactions in Fe, Ni and Co, J. Appl. Phys. **85**, 4827 (1999).

[11] W. Kohn and L. J. Sham, Self-consistent equations including exchange and correlation effects, Phys. Rev. **140**, A1133 (1965).

[12] U. von Barth and L. Hedin, A local exchange-correlation potential for the spin polarized case, J. Phys. C: Solid State Phys. **5**, 1629 (1972).

[13] F. Tran and P. Blaha, Accurate Band Gaps of Semiconductors and Insulators with a Semilocal Exchange-Correlation Potential, Phys. Rev. Lett. **102**, 226401 (2009).

[14] T. N. Lamichhane, V. Taufour, M. W. Masters, D. S. Parker, U. S. Kaluarachchi, S. Thimmaiah, S. L. Bud'ko, and P. C. Canfield, Discovery of ferromagnetism with large magnetic anisotropy in ZrMnP and HfMnP, Appl. Phys. Lett. **109**, 092402 (2016).

[15] A. F. May, Y. Liu, S. Calder, D. S. Parker, T. Pandey, E. Cakmak, H. Cao, J. Q. Yan, and M. A. McGuire, Magnetic order and interactions in ferrimagnetic $Mn_3Si_2Te_6$, Phys. Rev. B **95**, 174440 (2017).

[16] T. J. Williams, A. E. Taylor, A. D. Christianson, S. E. Hahn, R. S. Fishman, D. S. Parker, M. A. McGuire, B. C. Sales, and M. D. Lumsden, Extended magnetic exchange interactions in the high-temperature ferromagnet MnBi, Appl. Phys. Lett. **108**, 192403 (2016).

[17] G. D. Samolyuk, B. P. T. Fokwa, R. Dronskowski, and G. J. Miller, Phys. Rev. B **76**, 094404 (2007).

[18] M. A. McGuire, H. Cao, B. C. Chakoumakos, and B. C. Sales, Symmetry-lowering lattice distortion at the spin reorientation in MnBi single crystals, Phys. Rev. B **90**, 174425 (2014).

[19] D. S. Parker, Strong 3D and 1D magnetism in hexagonal Fe-chalcogenides FeS and FeSe vs. weak magnetism in hexagonal FeTe, Sci. Rep. **7**, 3388 (2017).

[20] G. Kresse and J. Hafner, *Ab initio* molecular dynamics for liquid metals, Phys. Rev. B **47**, 558 (1993); *Ab initio* molecular dynamics for liquid metals, **49**, 14251 (1994).

[21] G. Kresse and J. Furthmuller, Computer code VASP, Vienna, Austria, 1999, Comput. Mater. Sci. **6**, 15 (1996).

[22] G. Kresse and J. Furthmuller, Efficient iterative schemes for *ab initio* total-energy calculations using a plane-wave basis set, Phys. Rev. B **54**, 11169 (1996).

[23] G. Kresse and D. Joubert, From ultrasoft pseudopotentials to the projector augmented-wave method, Phys. Rev. B **59**, 1758 (1999).

[24] J. P. Perdew, A. Ruzsinszky, I. Gabor, O. A. Csonka, G. E. Vydrov, L. A. Scuseria, X. Zhou, and K. Burke, Restoring the Density-Gradient Expansion for Exchange in Solids and Surfaces, Phys. Rev. Lett. **100**, 136406 (2008).

[25] A. L. Allred, Electronegativity values from thermochemical data, J. Inorg. Nucl. Chem. **17**, 215 (1961).

[26] T. Ohtani, H. Nishihara, and K. Koga, Structure refinement and physical properties of the V_3Te_4 phase, Solid State Comm. **71**, 1179 (1989).

[27] D. J. Young, W. W. Smeltzer, and J. S. Kirkaldy, Nonstoichiometry and thermodynamics of chromium sulfides, J. Electrochem. Soc. **120**, 1221 (1973).

[28] K. Ozawa *et al.*, Effect of pressure on the curie point of $Cr_{1-\delta}Te$, Phys. Status Solidi (a) **11**, 581 (1972).

[29] Y. Takemura, H. Suto, N. Honda, and K. Kakuno, Characterization of FeSe thin films prepared on GaAs substrate by selenization technique, J. Appl. Phys. **81**, 5177 (1997).

[30] F. Grønvold, H. Haraldsen, and J. Vihovde, Phase and structural relations in the system iron tellurium, Acta Chem. Scand. **8**, 1927 (1954).

[31] See, http://energy.gov/downloads/doe-public-access-plan.

[32] F. Ye, Y. Liu, R. Whitfield, R. Osborn, and S. Rosenkranz, J. Appl. Crystallogr. **51**, 315 (2018).

[33] T. M. Michels-Clark, A. T. Savici, V. E. Lynch, X. Wang, and C. M. Hoffmann, J. Appl. Crystallogr. **49**, 497 (2016).